

23 A quarter of all primary production on Earth occurs in large nutrient deplete oceanic gyres¹. Primary
24 production in these large biomes is mainly driven by the dominant marine cyanobacteria *i.e.*
25 *Prochlorococcus* and *Synechococcus*². Gyres are permanently thermally stratified, where a lack of upward
26 physical mixing poses a challenge for the microbial communities that inhabit them. How then do purely
27 planktonic cyanobacterial cells in suspension combat the downward pull of gravity through the biological
28 pump –*i.e.* drawing fixed carbon towards the ocean interior? Moreover, how do these highly-specialised
29 planktonic microbes place themselves in their ‘preferred spot’, such as the well-established vertical
30 distribution of high and low light-adapted *Prochlorococcus* ecotypes^{3–5}? Marine picocyanobacteria lack
31 flagellar structures for swimming or gas vacuoles for flotation⁶, and only a limited number of
32 *Synechococcus* strains possess non-conventional mechanisms for motility^{7,8}. Therefore, it has been assumed
33 that these free-living microbes avoid sinking due to their lower density and reduced size⁹, and bloom when
34 they encounter their optimal environmental conditions while drifting randomly within marine currents.

35 To date, type IV pili are known to provide functions such as twitching motility, surface attachment,
36 biofilm formation, pathogenicity, as well as conjugation, exogenous DNA acquisition and competence^{10–12}.
37 These extracellular appendages can be rapidly extended and retracted by polymerising and depolymerising
38 cycles of the major pilin subunit *e.g.* PilA, requiring a defined transmembrane apparatus and the
39 consumption of energy in the form of ATP^{11,13}. Functional analysis of most type IV pili has focused on
40 pathogenic microbes and their use of surfaces or substrates for pilus anchoring. However, analysis of pili
41 from freshwater cyanobacteria has revealed these appendages can be used for twitching motility during
42 phototaxis in *Synechocystis*¹⁴ or exogenous DNA acquisition in both *Synechocystis* and *Synechococcus*
43 *elongatus*^{15,16}. This latter function requires an additional set of proteins for competence such as ComEA and
44 ComEC. While acquisition of DNA by *S. elongatus* is performed by the third of three PilA-like proteins
45 encoded by this strain (PilA3)¹⁶, no known function has been attributed to PilA1 and PilA2 other than being
46 dispensable for attachment and biofilm formation¹⁷. A mutant in *S. elongatus* that no longer produced PilB
47 –the protein responsible for pilus elongation– abolished the production of pili appendages, made up of

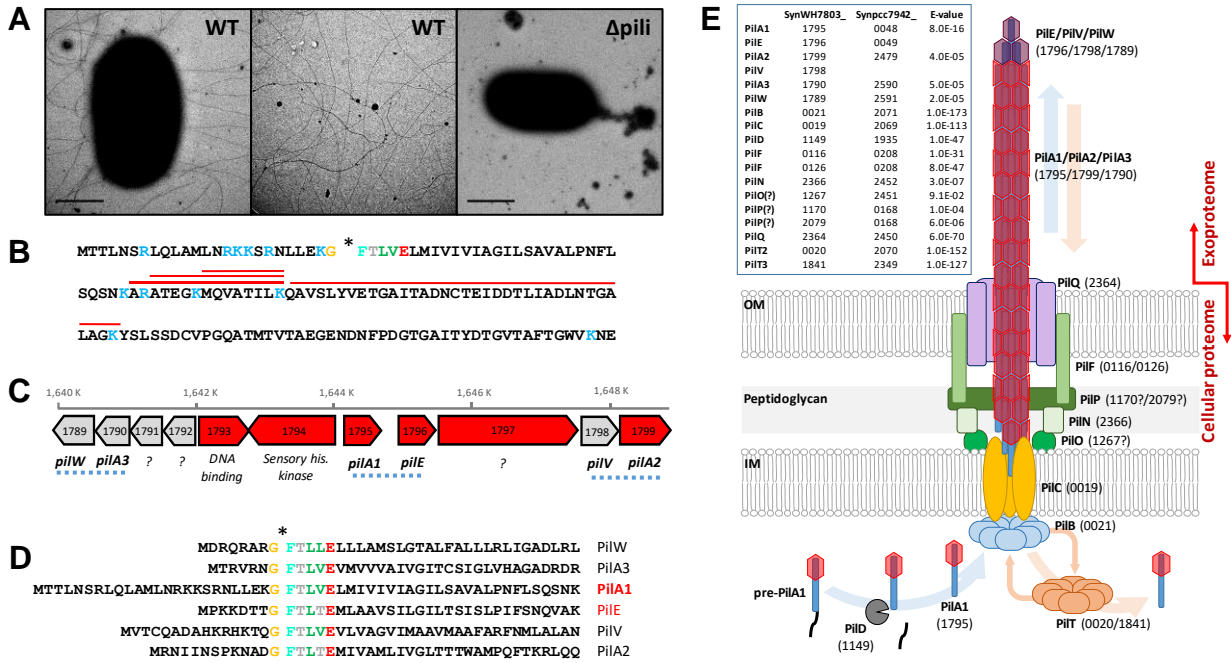
48 PilA1, and was reported to suppress planktonic growth of this strain¹⁷. The presence of pilus genes in purely
49 planktonic marine microbes has previously been reported, but their role remains enigmatic¹⁸.

50 Here, we show that almost a quarter of all marine picocyanobacteria encode a PilA1-like pilus. We
51 show that this extracellular appendage produced in these purely planktonic organisms –which rarely
52 encounter any kind of surface in their natural habitat– allows cells to increase drag and remain in an optimal
53 position in the water column as well as avoid being preyed upon. This provides yet another biological
54 function to these filamentous appendages and sheds light on the ecological role of type IV pili in marine
55 ecosystems.

56

57 **RESULTS AND DISCUSSION**

58 **Abundant production of a type IV pilus in *Synechococcus* sp. WH7803.** We first detected an abundant
59 PilA protein (*i.e.* SynWH7803_1795) in the extracellular proteomes of the model marine cyanobacterium
60 *Synechococcus* sp. WH7803, accounting for up to 25% of the exoproteome^{19,20}. Transmission electron
61 microscopy confirmed the existence of the macromolecular pili structures (Fig 1A and Fig S1). Unlike
62 *Synechocystis* sp. PCC6803 that simultaneously produces thick and thin pili¹⁴, this marine
63 picocyanobacterium presented multiple pili of similar thickness, each ~10 μm in length. The amino acid
64 sequence of PilA revealed a typical type II secretion signal and a conserved GFTLxE motif at the N-
65 terminus of the protein (Fig 1B) that is known to be cleaved in the cytoplasm before the protein is
66 translocated to the base of the pili for assembly¹⁰. After cleavage, the N-terminal of PilA can be post-
67 translationally modified, *e.g.* methylated, to increase the hydrophobicity and stability of the pilin^{10,21},
68 although we were unable to detect this modified N-terminus tryptic peptide during proteomic analyses. In
69 close proximity to *pilA* in the *Synechococcus* sp. WH7803 genome we found five other type IV-like pilin
70 genes (Fig 1C), all with the conserved GFTLxE motif (Fig 1D).



71

72 **Fig 1 | Pilus in the marine cyanobacterium *Synechococcus* sp. WH7803.** (A) Transmission electron microscopy images of wild type *Synechococcus* sp. WH7803 (WT) and pili mutant (Δ pili) obtained from
73 late exponential liquid cultures incubated in ASW medium under optimal growth conditions. Long pili
74 appendages were only observed in the wild type strain (Fig S1). Middle panel image, obtained with the
75 same magnification as other panels, is from an intercellular region between wild type cells to improve the
76 visualisation of the pili. Scale bar represents 1 μ m. (B) The amino acid sequence of PilA1
77 (SynWH7803_1795). Trypsin hydrolytic sites are indicated in blue. Red lines highlight tryptic peptides
78 detected by shotgun proteomics. The conserved GFTLxE motif is shown and the cleavage site is indicated
79 with an asterisk. (C) Genomic context of *pilA1* in *Synechococcus* sp. WH7803. Numbers in each gene
80 represent their ID number (SynWH7803_). In red are genes detected by proteomics. While PilA1 and PilE
81 are abundantly detected in exoprotoomes²⁰, PilA2 has only ever been detected in cellular proteomes of this
82 strain²². Blue dotted lines indicate genes encoding possible structural pilin pairs, *i.e.* PilA1-PilE, PilA2-
83 PilV and PilA3-PilW. Question marks indicate genes encoding proteins of unknown function. (D) The N-
84 terminal amino acid sequence of PilA1 and five other pilin-like proteins, all with the highly conserved
85 GFTLxE motif. (E) *Synechococcus* sp. WH7803 structural pilus proteins identified by homology with *S.*
86 *elongatus* PCC 7942¹⁶ and assembled as modelled by Craig *et al*¹¹.
87
88

89

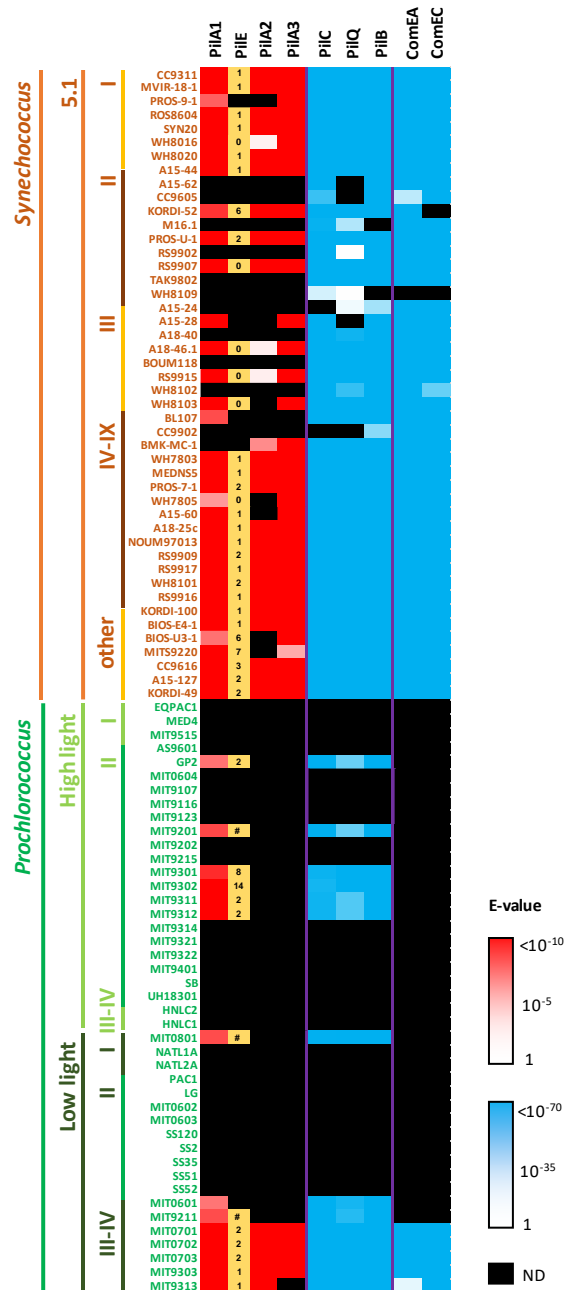
90 Using the pilus apparatus from the freshwater cyanobacterium *S. elongatus* PCC 7942 as a
91 reference¹⁶ and the established architecture for type IV pilus machinery¹¹, we were able to find all
92 components necessary for pilus assembly in *Synechococcus* sp. WH7803 (Fig 1E). The genetic cluster
93 encoding the six pilin-like proteins (Fig 1C and 1D) likely produces three types of pili that use the same
transmembrane pilus structure. Based on homology with the annotated genes from *S. elongatus*¹⁶ and

94 conserved domains found using the CD-search tool in NCBI, we suggest the three pili types: PilA1-PilE,
95 PilA2-PilV and PilA3-PilW (Fig 1C). Of these types, shotgun proteomic analyses have only ever detected
96 PilA1-PilE^{19,20}, although PilA2 was also detected in low abundance in cellular –but not extracellular–
97 proteomic datasets²². Unlike in *S. elongatus*, where PilA1 and the contiguously-encoded pilin-like protein
98 are almost identical, the amino acid sequence of PilA1 and PilE in *Synechococcus* sp. WH7803 are clearly
99 distinguishable. Although in much lower abundance, PilE seems to be correlated with PilA1 in the
100 exoproteomes of this cyanobacterium^{19,20} and, therefore, it is possible that PilE and PilA1 form subunits of
101 the same pilus apparatus.

102

103 **Pilus distribution amongst picocyanobacterial isolates and Single-cell Assembled Genomes (SAGs).**

104 Genomic analysis of sequenced marine picocyanobacterial isolates downloaded from the Cyanorak
105 database revealed that 74% of sequenced *Synechococcus* (n=46) and 33% of *Prochlorococcus* (n=43)
106 encoded *pilA1* (Fig 2 and Table S1). In *Synechococcus*, the pilus was prevalent in all clades (93%; n=28)
107 except for clades II and III where it was less abundant (44%; n=18). Interestingly, all low light
108 *Prochlorococcus* isolates from clades III and IV encoded *pilA1* (n=7; Fig 2). Most of these *pilA1*-containing
109 strains also encoded a *pilE* homologue in close proximity. Genes *pilA2* and *pilA3* were also abundantly
110 found in *Synechococcus* (59 and 74%, respectively), although were much less prevalent in *Prochlorococcus*
111 (12 and 9%, respectively). As expected, all strains that encode at least one of the *pilA* types also possessed
112 the transmembrane pilus apparatus, whereas this apparatus was completely absent or partially lost in strains
113 lacking *pilA* (Fig 2). PilA3 is known to be involved in DNA uptake and competence in *S. elongatus*,
114 requiring additional competence proteins to do so¹⁶. Marine picyanobacteria are not known for being
115 naturally competent but, interestingly, all strains encoding PilA3 also contained the competence genes
116 encoding ComEA and ComEC (Fig 2). Further work is needed to investigate the conditions under which
117 the PilA3-type pilus becomes active in these organisms and, therefore, when exogenous DNA might be
118 taken up.



119

120 **Fig 2 | The presence of pilus-related proteins in cultured marine picocyanobacteria strains.** Pilus

121 proteins from *Synechococcus* sp. WH7803 were used for the BLASTp search. Log10 E-value scales are

122 shown (1 to $<10^{-10}$, white to red; and 1 to $<10^{-70}$, white to blue). Black cells represent proteins that were not

123 detected (ND). Numbers in the 'Pile' column indicate the genomic distance between *pilE* and *pilA1*

124 homologues (e.g. 1 denotes *pilE* and *pilA1* are contiguous in the genome; 0 denotes the same gene gave

125 homology to both *pilE* and *pilA1* due to the conserved N-terminal of the protein; # denotes both genes are

126 separated by >20 genes). PilC, PilQ and PilB were used to determine the presence of the pilus

127 transmembrane apparatus. ComEA and ComEC were selected to determine the presence of the additional

128 machinery required for competence.

129

130 The GFTLxE motif is conserved in 87.5% of PilA1 sequences encoded by cultured marine
131 picocyanobacteria (*i.e.* 42 of the 48 sequences; Table S1). The remaining six PilA1 sequences possess a
132 GFSLxE motif, five of which were in *Prochlorococcus* strains. Across the full length of the mature PilA1
133 protein, which on average is 140 amino acids long, only the first ~50 N-terminal amino acids starting from
134 the conserved GFTLxE motif are well conserved amongst all sequences, a commonly observed feature in
135 PilA-like proteins¹¹. The C-terminus of the protein showed a remarkably high variability even between
136 closely related strains. Despite this high variability, their predicted structures were still similar to those of
137 known pili subunits (Fig S2)^{23,24}. During pili assembly, the helix encoded by the conserved N-terminus of
138 PilA remains in the pilus core and only the variable C-terminus –that producing anti-parallel β -sheets– is
139 exposed to the milieu¹¹. We hypothesise that the hyper-variability of the exposed C-terminus is a strategy
140 to escape phage attachment, it being a known pathway used by phage for host encounter and infection^{25,26}.
141 Similarly, flagella have a hyper-variable region, which has also been attributed to phage and immune system
142 evasion²⁷.

143 The screening of 190 picocyanobacterial Single-cell Assembled Genomes (SAGs) obtained from
144 surface seawater across the globe²⁸ –those with over 75% completeness– revealed the presence of *pilA1*
145 and genes encoding components of the pilus apparatus in almost one in four marine picocyanobacteria (24%
146 encoded *pilA1* and 21-25% the pilus apparatus; Table 1 and Table S1). As expected by its abundance in the
147 oceans, *Prochlorococcus* comprised almost 96% of all 190 SAGs (Table 1). The prevalence of the pilus
148 was much higher amongst the low light *Prochlorococcus* SAGs from clades II/III (67-80%) than in those
149 belonging to other ecotypes, and *Synechococcus* showed the abundance observed in cultures isolates
150 (~76%; Table 1).

151

152

153

154

155 **Table 1** | PilA1 and pilus apparatus distribution amongst planktonic marine SAGs.

	# SAGs ^a	Compl. ^b	PilA1 ^c	PilC ^c	PilQ ^c	PilB56
Total	190	87%	39 (24%)	39 (24%)	35 (21%)	42 (25%)
<i>Prochlorococcus</i>						
HL I	23	89%	4 (20%)	5 (24%)	3 (15%)	5 (24%)
HL II	98	88%	12 (14%)	12 (14%)	12 (14%)	13 (15%)
HL IV	5	88%	1 (23%)	1 (23%)	1 (23%)	1 (23%)
LL I	28	87%	6 (25%)	5 (21%)	7 (29%)	6 (23%)
LL II/III	9	83%	6 (80%)	5 (67%)	5 (67%)	5 (61%)
Unclassified	19	86%	5 (31%)	4 (24%)	4 (24%)	4 (24%)
<i>Synechococcus</i>	8	82%	5 (76%)	7 (100%)	3 (46%)	8 (100%)

164 ^a Total number of available SAGs with >75% genome completeness and for which the phylogeny had been assigned.

165 ^b SAGs average genome completeness

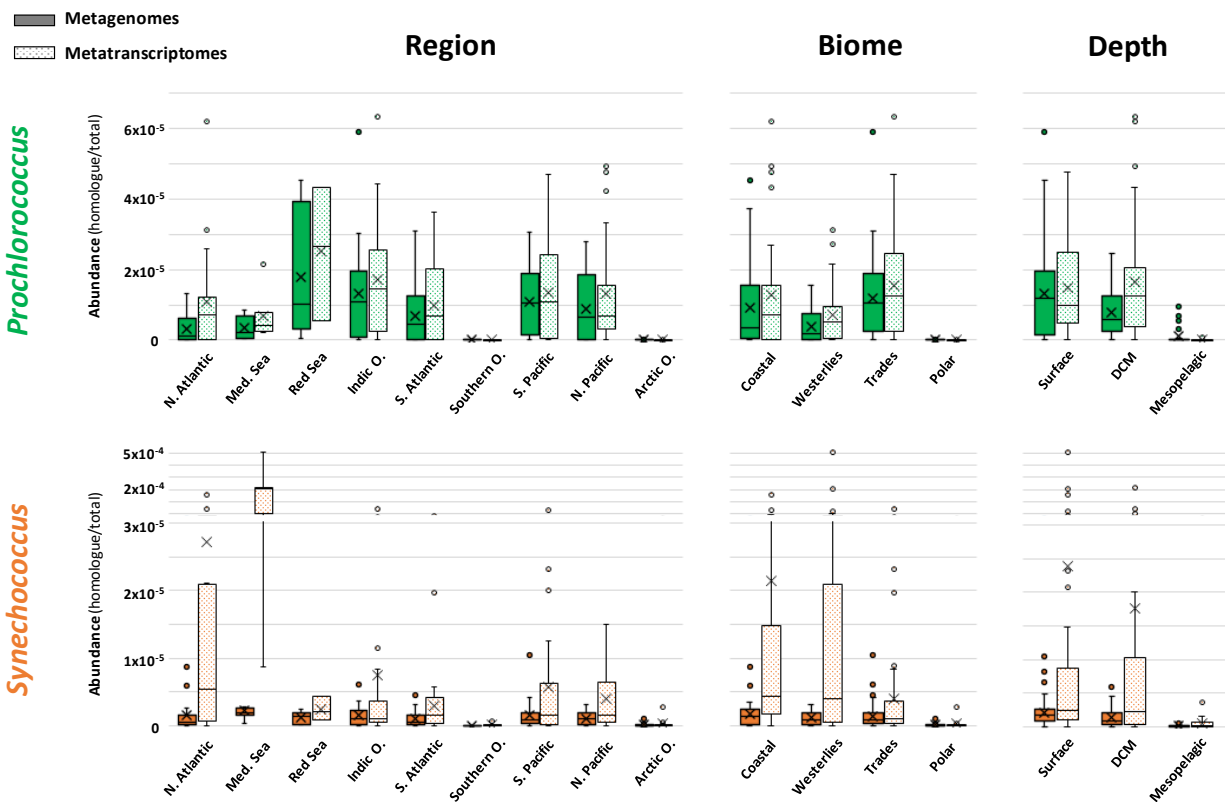
166 ^c Number of SAGs encoding for the pilus proteins. The prevalence in each group is shown as the percentage of SAGs encoding
167 each protein corrected by the average genome completeness.

168

169 **Global distribution and expression of picocyanobacterial *pilA1* in marine pelagic ecosystems.** The
170 distribution and expression of *pilA1* in the surface ocean was determined by analysing its presence in the
171 global marine TARA metagenome and metatranscriptome datasets. An HMM profile generated from the
172 PilA1 sequences (cultured isolates and SAGs; Table S1) was used to search the TARA datasets in the Ocean
173 Gene Atlas portal²⁹ retrieving 903 and 837 individual hits from the metagenomes and metatranscriptomes,
174 respectively (using a cut-off E-value < 10⁻¹⁰). Sequences assigned to *Prochlorococcus* represented 85% in
175 both datasets, whereas those assigned to *Synechococcus* represented 12% and 11% of the metagenomes and
176 metatranscriptomes, respectively. BLAST analysis of these hits against PilA1, PilA2 and PilA3 sequences
177 was used to confirm the specificity of our HMM profile, proving effective in discriminating against PilA2
178 and PilA3 sequences (each representing less than 1% of the hits).

179 The abundance and transcription of genes encoding PilA1 from *Prochlorococcus* and
180 *Synechococcus* across all oceanic regions, marine biomes and water depths (Fig 3) revealed a similar
181 abundance of *pilA1* from *Prochlorococcus* in both metagenomic and metatranscriptomic datasets. In
182 contrast, *pilA1* from *Synechococcus* was enriched in the metatranscriptomes, mainly driven by the increased
183 expression in the North Atlantic Ocean and Mediterranean Sea as well as in coastal and westerlies, biomes
184 where *Synechococcus* are known to thrive. As expected, a large reduction in the presence and expression
185 of the picocyanobacterial *pilA1* was noted in the polar oceans, where both genus are not abundant.
186 Furthermore, the presence and transcription of cyanobacterial *pilA1* decreased drastically in the aphotic

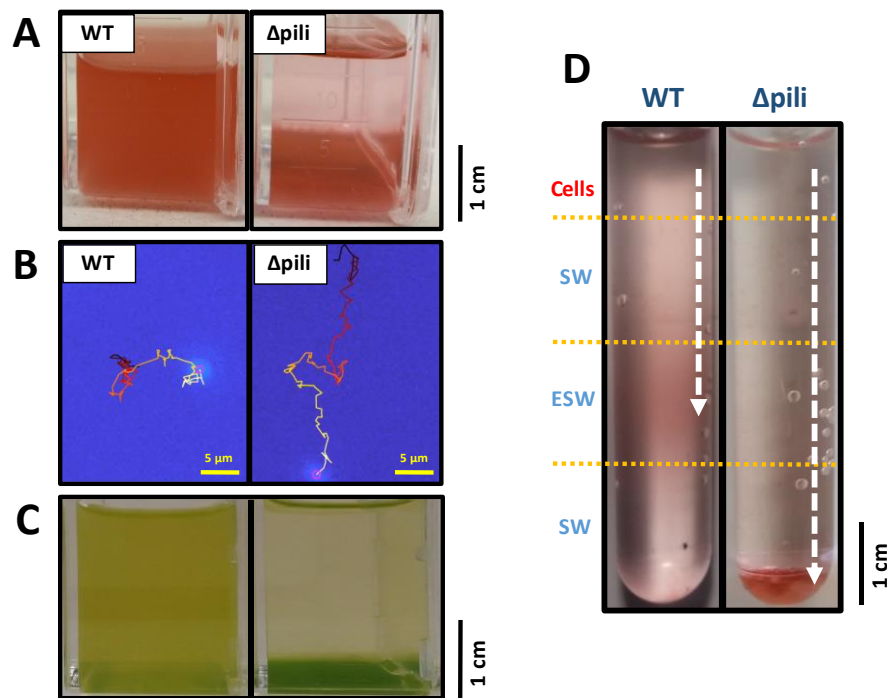
187 mesopelagic layer, in accordance with picocyanobacteria naturally populating only euphotic layers of the
 188 ocean.
 189



190
 191 **Fig 3 | Distribution of PilA1 amongst marine ecosystems.** Whisker box plots showing *pilA1* gene
 192 abundance in *Prochlorococcus* and *Synechococcus* in metagenomes and metatranscriptomes generated
 193 from all filters (0.2-3 μm) and sampling stations of the TARA Oceans global marine survey. Abundance
 194 was calculated by dividing the sum of the abundances of *pilA1* homologs assigned to each genus by the
 195 sum of total gene abundance from all reads from the sample. Data is presented by oceanic region, biome
 196 and water depth *i.e.* surface, deep chlorophyll maxima (DCM) and mesopelagic layers. Filters from polar
 197 regions were excluded from the depth abundance analysis. Exclusive median (line), average (cross) and
 198 atypical values (circles) are also indicated.

199
 200 **PilA1-type pili increase drag and allow cells to remain planktonic.** The extensive distribution and
 201 expression of such an extracellular appendage begs the question why such a complex structure is so
 202 prevalent in such streamlined planktonic cyanobacteria. To assess this, and to assign a biological function
 203 to this extracellular structure in the context of the ecology of marine planktonic bacteria more generally,

204 we abolished the production of PilA1 and PilE in *Synechococcus* sp. WH7803. As expected, the fully
205 segregated pili mutant strain no longer produced the extracellular structure (Fig 1A and Fig S1). Most
206 remarkably, we observed a clear loss in the strain's ability to remain suspended in its typical planktonic
207 form (Fig 4A). By tracking wild type and pili mutant cells of *Synechococcus* sp. WH7803, we determined
208 that the lack of pili produced an average cell sinking rate of 8.4 ± 0.4 mm/day, while the wild type had an
209 average uplifting drift of 0.8 ± 0.3 mm/day (Fig 4B, Suppl. Movies 1-4 and full data in Table S2). While
210 avoiding sedimentation, the pili did not appear to confer motility, with both mutant and wild type strains
211 producing 'pin-prick' colonies in sloppy agar plates as opposed to fuzzy colonies characteristic of motile
212 strains⁸. Furthermore, neither the mutant nor the wild type strain aggregated when grown in shaken liquid
213 cultures.



214
215 **Fig 4 | Pili avoid sinking in planktonic marine picocyanobacteria.** (A) Non-shaken cultures of wild type
216 (WT) and pili mutant (Δ pili) of *Synechococcus* sp. WH7803. The pili mutation and phenotype has proven
217 very stable with the mutant strain unable to remain in a planktonic form when not shaken. The appearance
218 of the mutant in the image is consistently achieved after 2-3 days of no shaking. (B) Example of tracked
219 suspended cell from a wild type and pili mutant culture of *Synechococcus* sp. WH7803. The movement was
220 tracked over 100 s and movement is indicated from dark red (start) to yellow (end). Full data of all tracked
221 cells can be found in Table S2 and examples in Movies S1-S4. (C) Non-shaken *Prochlorococcus* sp.
222 MIT9313 cultures grown in Pro99 medium (left) and PCR-S11 medium (right). The appearance of cells in

223 the image is consistently achieved after 2-3 days of no shaking. PilA1 (PMT_0263) was only detected in
224 the exoproteome of suspended cultures (left; Table S4). (D) Nutrient step gradient column where wild type
225 and pili mutant cells of *Synechococcus* sp. WH7803 were placed at the top. Nutrient deplete (SW) and
226 nutrient enriched layers (ESW) are indicated. Cells were harvested by centrifugation from late-exponential
227 cultures grown under optimal conditions, and resuspended in SW. The arrow indicates the trajectory made
228 by the cells, and where they accumulated after three days. Other gradients tested are shown in Fig S4.
229 Images represent one of three culture replicates.
230

231 We performed a comparative proteomic analysis between wild type *Synechococcus* sp. WH7803
232 and the pili mutant to assess any additional effects of disrupting the PilA1-PilE pilus (Table S3). Apart from
233 the complete absence of the PilA1 and PilE proteins, only three other proteins were significantly down-
234 regulated in the cellular proteome of the pili mutant strain (Fig S3): SynWH7803_0049 (12.9 fold) and
235 SynWH7803_1797 (3.2 fold), both of unknown function and, most interestingly the pilus retraction protein
236 PilT (SynWH7803_0020; 2.9 fold reduction). SynWH7803_1797 is located just downstream of PilA1-PilE
237 and is predicted to encode a secreted protein that is usually found in low abundance in the exoproteome of
238 *Synechococcus* sp. WH7803²⁰. Indeed, it was also found down-regulated in the exoproteome of the pili
239 mutant (2.5x; Fig S3). The exoproteomes also revealed a generalised shift of proteins more abundantly
240 detected in the pili mutant. These were mainly low abundance cytoplasmic proteins that were barely
241 detected in the wild type strain (Fig S3 and Table S3). Most likely, the absence of the abundant PilA1
242 protein from the exoproteome of the mutant strain caused an artifactual increase in the detection of lower
243 abundance proteins by mass spectrometry and, despite efforts to normalise the data, there was an apparent
244 upregulation of most proteins.

245 We had previously observed that *Prochlorococcus* sp. MIT9313 (a strain that encodes PilA1; Fig
246 2) routinely switches between planktonic and sedimenting lifestyles when grown in different media (Pro99
247 and PCR-S11, respectively; Fig 4C). Whilst *Prochlorococcus* remains genetically intractable³⁰, we
248 compared the exoproteomes of this strain in both medias. Commensurate with our findings in
249 *Synechococcus* sp. WH7803, PilA1 was not detected in the exoproteomes of sedimenting *Prochlorococcus*
250 sp. MIT9313 cultures, whereas it was present in all of the planktonic ones (*i.e.* PMT_0263; Table S4),

251 suggesting *Prochlorococcus* can coordinate production of the pili in response to the distinct nutrient
252 environments present in both medias.

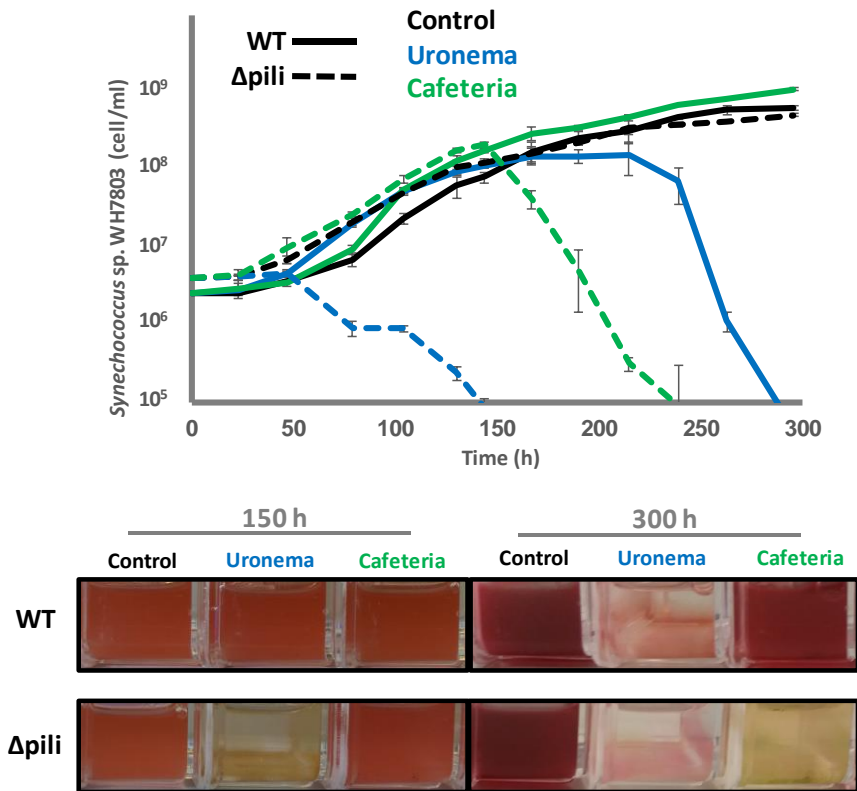
253

254 **PilA1 allows cells to retain an optimal position within the water column.** We further explored the effect
255 of nutrient stress on pili production in *Synechococcus* sp. WH7803, with nitrogen and metal depletion
256 showing the strongest decline (*i.e.* 11.5 and 3.4-fold decrease in PilA1 production, respectively), whilst
257 phosphorus depletion had no effect (Table S5). Although in low abundance, PilA1 of *Synechococcus* sp.
258 WH7803 was detected even under natural oligotrophic conditions (*i.e.* when incubated in natural seawater;
259 representing 0.3% of the exoproteome) and showed a slight increase after adding environmentally-relevant
260 concentrations of nutrients (0.5% of the exoproteome in the presence of 8.8 μM N and 0.18 μM P). Pili
261 detection became most obvious under higher nutrient conditions (60-fold increase in pili at 88 μM N and
262 1.8 μM P when compared to nutrient deplete seawater; Table S6). Considering the biological significance
263 of this phenotype in the context of marine planktonic organisms –where the production of pili reduces
264 sedimentation by increasing the viscous drag of the cell– the extension/retraction of pili would allow a cell
265 to position itself at an optimal position in the water column, *e.g.* in patches of high nutrient availability. To
266 further investigate this, we set up a nutrient step gradient. While the pili mutant, as expected, sank through
267 the gradient independently of nutrient availability, the wild type strain was able to position itself in the
268 nutrient-replete layer where it remained via the production of pili (Fig 4D and Fig S4).

269 *Synechococcus* sp. WH7803 also retained pili over a 24 h period of darkness. Nevertheless, after
270 three days under dark conditions –during which cultures are known to remain viable³¹, the detection of pili
271 dropped drastically (*i.e.* >20-fold drop in pili abundance in the exoproteome; Table S7). Marine
272 cyanobacteria occupying photic layers of the ocean will therefore keep their pili structures over normal
273 diurnal light-dark cycles to maintain their position, but cells will cease to retain their position once they
274 sink out of the euphotic zone, retracting their pili possibly as a strategy to recover energy while awaiting an
275 uplift back to photic layers by upwelling currents.

276

277 **Pili prevent grazing.** Given the cell surface nature of this pilus, we also assessed whether it could mediate
278 ecological interactions with other organisms. We found that as well as preventing sedimentation, pili allow
279 bacteria to evade predation by protist grazers. Thus, *Synechococcus* sp. WH7803 and the pili mutant grown
280 in the presence of two bacterivorous protozoa *i.e.* the preying ciliate *Uronema* and suspension feeding
281 flagellate *Cafeteria*, strikingly showed that whilst the wild type strain was able to completely evade grazing
282 by *Cafeteria* and largely delay culture depletion by *Uronema*, the pili mutant was efficiently grazed by both
283 protists (Fig 5). Presumably, the long pili appendages interfere with the way bacterivorous protozoa access
284 their prey and, hence, this reduces their susceptibility to grazing.



285

286 **Fig 5 | Pili confer resistance to grazing.** Growth curves (top panel) and culture images (bottom panel) of
287 wild type (WT) and pili mutant (Δ pili) cultures of *Synechococcus* sp. WH7803 incubated in the absence
288 (control) and presence of two different grazers. Cultures were subjected to constant shaking to keep the
289 wild type and PilA1 mutant in planktonic form. Error bars represent the standard deviation from three
290 culture replicates. Images represent one of three culture replicates.

291

292

293 **Concluding remarks**

294 Together, our data suggests a novel and sophisticated mechanism that enables oligotrophic marine
295 picocyanobacteria to stay buoyant and reduce cell death due to grazing through the use of pili, adding a
296 new biological function to these extracellular appendages. This PilA1-type pilus, widely distributed and
297 expressed amongst dominant marine oligotrophic cyanobacteria, allow these purely planktonic organisms
298 to increase cell drag and, consequently, maintain an optimal position in the water column. This mechanism
299 is under tight regulation in response to discrete stimuli *e.g.* nutrients, which may vary depending on the
300 ecological adaptation and preferred niche of each individual organism. Therefore, as opposed to flagellated
301 bacteria that show positive chemotaxis towards nutrient hotspots in the oceans³², non-motile
302 picocyanobacteria may apply a more passive strategy which consists of elongating their pili when they
303 encounter preferable conditions to remain in an optimal position while drifting in a water body. These long
304 appendages also interfere with the access of bacterivorous protozoa to their prey allowing pili-producing
305 cells to evade grazing. Further research should define: i) the biophysical differences between pili that allow
306 attachment and floatation, ii) the resources required for this floatation system and advantages over other
307 mechanisms such as flagella, and iii) the ecological trade-offs of having such extracellular appendages.
308 Thus, besides being beneficial, pili could also be a handicap to those cells that produce them as, being phage
309 binding sites^{25,26}, they will increase the chance of interacting with phage and hence their susceptibility to
310 phage infection.

311 The biological carbon pump and microbial loop pose important challenges for streamlined marine
312 cyanobacteria, which have moved away from canonical flagellar motility and have evolved this more
313 passive mechanism for floatation that may require less resources and no additional convoluted tactic systems.
314 This discovery changes our ecological perception of this dominant marine bacterial group, and will have
315 important consequences for our future understanding of predator-prey and carbon flux dynamics in the
316 oceans.

317

318

319 **Methods**

320 *Culture conditions*

321 *Synechococcus* sp. WH7803 was grown in ASW medium and oligotrophic seawater using conditions
322 previously described²². Experiments were performed using 20 ml cultures contained in 25 cm² rectangular
323 cell culture flasks (Falcon) with vented caps. Cultures were incubated under optimal growth conditions *i.e.*
324 at 22°C at a light intensity of 10 μmol photons m⁻² s⁻¹ with shaking (140 r.p.m.), unless otherwise stated in
325 the text. To study the influence of nutrients on pili production, media was prepared by i) not adding different
326 nutrient sources into ASW media, *i.e.* nitrogen, phosphorus and trace metals, or ii) diluting ASW in
327 oligotrophic seawater (*i.e.* 1:1000, 1:100 and 1:10). The low light-adapted ecotype *Prochlorococcus* sp.
328 MIT9313 was grown in 40 ml Pro99 medium and PCR-S11 medium with no additional vitamins³³. Different
329 light intensities (*i.e.* 4 and 15 μmol photons m⁻² s⁻¹) and temperatures (*i.e.* 14 and 22°C) were tested.
330 Cyanobacterial culture growth was routinely monitored by flow cytometry (BD Fortessa).

331 Grazing experiments were performed using ASW-washed *Uronema marinum* (isolated from Qingdao Bay)
332 and *Cafeteria roenbergensis* CCAP 1900/1 cells. Briefly, 10 ml culture was subjected to centrifugation at
333 4000g for 15 min and the pellet resuspended in 10 ml ASW. One ml of washed grazers was used to inoculate
334 20 ml cultures of wild type and pili mutant of *Synechococcus* sp. WH7803 at an initial concentration of 3-
335 4 x 10⁶ cells ml⁻¹. Triplicates cultures were incubated under optimal conditions, including shaking to avoid
336 pili mutant sedimentation (see above).

337

338 *Pilus knockout mutant in Synechococcus sp. WH7803*

339 Genes SynWH7803_1795 and SynWH7803_1796 (*pilA1* and *pilE*, respectively) were replaced by a
340 gentamicin cassette via a double recombination event to generate the *Synechococcus* sp. WH7803 pili
341 mutant. Two flanking regions of 700 bp from the genome of *Synechococcus* sp. WH7803 and the
342 gentamicin cassette from pBBR-MCS³⁴ were amplified by PCR using primers indicated in Table M1, and
343 inserted into vector pK18mobsacB³⁵ using the Gibson assembly method following manufacturer's
344 instructions (New England Biolabs). The detailed protocol to generate mutants in *Synechococcus* sp.
345 WH7803 is given in the Supplementary Information. All three transconjugant colonies that were picked
346 had the same sinking phenotype, had doubly recombined (as checked by sequencing the overlapping
347 regions) and were fully segregated. One mutant was subsequently selected to make axenic by eliminating
348 the 'helper' strain and used for further experimentation. The pilus mutation is stable and has retained its
349 sinking phenotype over time.

350

351 *Transmission Electron Microscopy*

352 Optimally-grown *Synechococcus* sp. WH7803 and pilus mutant cultures were fixed using 3% (v/v) final
353 concentration glutaraldehyde after which 5 μ l were delicately transferred onto a glow-discharge
354 formvar/carbon coated grid and left 2-3 min for cells to attach. After blotting the excess media, negative
355 staining was achieved by applying a drop of 2% uranyl acetate to the grid for 1 min. The excess stain was
356 blotted off and left to air dry before imaging using a JEOL 2011 TEM with Gatan Ultrascan.

357

358 *Tracking and imaging of sinking cells*

359 The movement of wild type *Synechococcus* sp. WH7803 and pilus mutant through a nutrient step gradient
360 was performed by placing washed cells in oligotrophic SW on top of a column where nutrient layers
361 (nutrient deplete and amended layers as indicated, using ASW media) were achieved by increasing sucrose
362 concentration (*i.e.* 2.5% w/v per layer).

363 Sedimentation tracking and velocity measurements were conducted using a setup as previously described³⁶.
364 Briefly, a sample chamber was prepared by gluing a square glass capillary (inner dimensions 1.00 x 1.00
365 mm, length 50 mm; CM Scientific, UK) onto a glass slide using an optical glue (#81; Norland, USA).
366 Tubings (Masterflex Transfer Tubing, Tygon® ND-100-80 Microbore, 0.020" ID x 0.060" OD; inner
367 dimension 0.51 mm; Cole-Parmer, USA) were attached to both ends of the sample chamber using blunt
368 dispensing nozzle tips (Polypro Hubs; Adhesive Dispensing, UK), one-way stopcock valves (WZ-30600-
369 00; Cole-Parmer, USA), and Luer connectors. *Synechococcus* was pulled into the capillary through the inlet
370 by manual suction using a 2 ml syringe connected to the outlet of the capillary system. After introducing
371 the sample, the microfluidic system was isolated by closing the stopcock valves. Samples were left to settle
372 for 30-60 minutes before recording. The slide-capillary system was held vertically by an adjustable
373 translation stage (PT1B/M; Thorlabs, USA), and placed between a white LED ring light source and a
374 continuously focusable objective (InfiniProbe TS-160; Infinity Photo-Optical Company, USA) for dark-
375 field imaging. Images were acquired with magnification set at 16 \times , using a CMOS FLIR Grasshopper3
376 (GS3-U3-23S6M-C; Point Grey Research Inc., Canada) operated with FlyCapture2 (FLIR Systems UK).
377 Recordings were done at 1 fps for either 1, 2, or 5 minutes. The system was calibrated with a resolution
378 target (R2L2S1P Positive NBS 1963A; Thorlabs, USA). Sedimentation velocities were calculated with
379 custom-made codes in MATLAB 2019a, based on particle tracking code from Crocker and Grier³⁷. Briefly,
380 features corresponding to individual cells were selected based on shape and image intensity, and the

381 distribution of frame-to-frame displacements was calculated from all the tracks lasting at least 20s. All the
382 experiments were checked for outliers.

383

384 *Proteome preparation and shotgun analysis*

385 20 ml cell cultures were subjected to centrifugation at 4000g for 15 min at 4°C. Cell pellets were used for
386 cell proteome analyses whereas the supernatants, which were further filtered to remove any remaining cells
387 (0.22 µm), were used for exoproteomic analyses. Exoproteomes were concentrated using a trichloroacetic
388 acid precipitation protocol as previously described³⁸. Cell pellets and exoproteome precipitates were
389 resuspended using 1x LDS buffer (ThermoFisher) containing 1% beta-mercaptoethanol and prepared for
390 LC-MS/MS via an in-gel trypsin digestion as described previously³⁸. Tryptic peptides were analysed with
391 an Orbitrap Fusion mass spectrometer (Thermo Scientific) coupled to an Ultimate 3000 RSLCnano system
392 (Dionex), using conditions described in Christie-Oleza et al³⁹. Mass spectra were identified using
393 *Synechococcus* sp. WH7803 and *Prochlorococcus* sp. MIT9313 UniProt databases (downloaded on
394 09/11/2017) and quantified using default parameters in MaxQuant v1.6.10.43⁴⁰. Comparative proteomic
395 analyses were performed using MS intensity values in Perseus v1.6.2.2⁴¹.

396

397 *In silico analysis of pilus proteins*

398 Major pilin proteins and pilus machinery were searched in *Synechococcus* sp. WH7803 using reference
399 proteins from *S. elongatus* PCC 7942¹⁶ and proposed modelled structure¹¹. Genomes from cultured
400 picocyanobacteria (*Synechococcus*, n=46, and *Prochlorococcus*, n=43) were downloaded from Cyanorak
401 and re-annotated using PROKKA vs. 1.7⁴². Genomes were then screened for the presence of PilA-like
402 proteins, structural proteins PilQ, PilB and PilC, and competence proteins ComEA and ComEC, via a local
403 BLAST server using the amino acid sequences from *Synechococcus* sp. WH7803.

404 The 190 picocyanobacterial SAGs from Berube *et al*²⁸, all with over 75% estimated genome completeness,
405 were downloaded and annotated in-house using PROKKA vs. 1.7. Annotated SAGs were screened for pilus
406 associated proteins using those from *Synechococcus* sp. WH7803 (Table S1), with further verification using
407 the Conserved Domain search tool from NCBI and manual curation in order to eliminate redundant matches
408 within each SAG and select PilA1-like proteins which had a PilE-like protein encoded in close proximity
409 in the genome.

410 The PilA1 sequences obtained from the cultured isolates and SAGs were used to generate an HMM profile
411 in Unipro UGENE vs. 33⁴³ implemented with the hmmbuild programme from HMM3⁴⁴ using the default
412 parameters. The resulting HMM profile was used to search the TARA oceans metagenomes and
413 metatranscriptomes via the functions offered in the Ocean Gene Atlas portal²⁹.

414 The modelled 3D protein structure of PilA-like proteins was performed with mature sequences using the I-
415 TASSER server's default settings⁴⁵.

416

417 **References**

- 418 1. Field, C. B., Behrenfeld, M. J., Randerson, J. T. & Falkowski, P. Primary production of the
419 biosphere: integrating terrestrial and oceanic components. *Science*. **281**, 237–240 (1998).
- 420 2. Jardillier, L., Zubkov, M. V, Pearman, J. & Scanlan, D. J. Significant CO₂ fixation by small
421 prymnesiophytes in the subtropical and tropical northeast Atlantic Ocean. *ISME J.* **4**, 1180–1192
422 (2010).
- 423 3. West, N. J. & Scanlan, D. J. Niche-partitioning of *Prochlorococcus* populations in a stratified water
424 column in the eastern North Atlantic Ocean. *Appl. Environ. Microbiol.* **65**, 2585–2591 (1999).
- 425 4. Malmstrom, R. R. *et al.* Temporal dynamics of *Prochlorococcus* ecotypes in the Atlantic and Pacific
426 oceans. *ISME J.* **4**, 1252–1264 (2010).
- 427 5. Thompson, A. W. *et al.* Dynamics of *Prochlorococcus* diversity and photoacclimation during short-
428 term shifts in water column stratification at station ALOHA. *Front. Mar. Sci.* **5**, 1252–1264 (2018).
- 429 6. Scanlan, D. J. *et al.* Ecological genomics of marine picocyanobacteria. *Microbiol. Mol. Biol. Rev.*
430 **73**, 249–299 (2009).
- 431 7. Waterbury, J. B., Willey, J. M., Franks, D. G., Valois, F. W. & Watson, S. W. A cyanobacterium
432 capable of swimming motility. *Science*. **230**, 74–76 (1985).
- 433 8. McCarren, J. & Brahamsha, B. Transposon mutagenesis in a marine *Synechococcus* strain: isolation
434 of swimming motility mutants. *J. Bacteriol.* **187**, 4457–62 (2005).
- 435 9. Cermak, N. *et al.* Direct single-cell biomass estimates for marine bacteria via Archimedes' principle.
436 *ISME J.* **11**, 825–828 (2017).
- 437 10. Giltner, C. L., Nguyen, Y. & Burrows, L. L. Type IV pilin proteins: versatile molecular modules.
438 *Microbiol. Mol. Biol. Rev.* **76**, 740–772 (2012).
- 439 11. Craig, L., Forest, K. T. & Maier, B. Type IV pili: dynamics, biophysics and functional consequences.
440 *Nat. Rev. Microbiol.* **17**, 429–440 (2019).
- 441 12. Ellison, C. K. *et al.* Retraction of DNA-bound type IV competence pili initiates DNA uptake during

- 442 natural transformation in *Vibrio cholerae*. *Nat. Microbiol.* **3**, 773–780 (2018).
- 443 13. Chang, Y.-W. *et al.* Architecture of the type IVa pilus machine. *Science.* **351**, aad2001 (2016).
- 444 14. Bhaya, D., Bianco, N. R., Bryant, D. & Grossman, A. Type IV pilus biogenesis and motility in the
445 cyanobacterium *Synechocystis* sp. PCC6803. *Mol. Microbiol.* **37**, 941–951 (2000).
- 446 15. Yoshihara, S. *et al.* Mutational analysis of genes involved in pilus structure, motility and
447 transformation competency in the unicellular motile ccyanobacterium *Synechocystis* sp. PCC6803.
448 *Plant Cell Physiol.* **42**, 63–73 (2001).
- 449 16. Taton, A. *et al.* The circadian clock and darkness control natural competence in cyanobacteria. *Nat.*
450 *Commun.* **11**, 1688 (2020).
- 451 17. Nagar, E. *et al.* Type 4 pili are dispensable for biofilm development in the cyanobacterium
452 *Synechococcus elongatus*. *Environ. Microbiol.* **19**, 2862–2872 (2017).
- 453 18. Schuergers, N. & Wilde, A. Appendages of the cyanobacterial cell. *Life* **5**, 700–715 (2015).
- 454 19. Christie-Oleza, J. A., Armengaud, J., Guerin, P. & Scanlan, D. J. Functional distinctness in the
455 exoproteomes of marine *Synechococcus*. *Environ. Microbiol.* **17**, 3781–3794 (2015).
- 456 20. Kaur, A., Hernandez-Fernaund, J. R., Aguilo-Ferretjans, M. D. M., Wellington, E. M. & Christie-
457 Oleza, J. A. 100 Days of marine *Synechococcus-Ruegeria pomeroyi* interaction: A detailed analysis
458 of the exoproteome. *Environ. Microbiol.* **20**, 785–799 (2018).
- 459 21. Strom, M. S., Nunn, D. N. & Lory, S. A single bifunctional enzyme, PilD, catalyzes cleavage and
460 N-methylation of proteins belonging to the type IV pilin family. *Proc. Natl. Acad. Sci. U. S. A.* **90**,
461 2404–2408 (1993).
- 462 22. Christie-Oleza, J. A., Sousoni, D., Lloyd, M., Armengaud, J. & Scanlan, D. J. Nutrient recycling
463 facilitates long-term stability of marine microbial phototroph-heterotroph interactions. *Nat.*
464 *Microbiol.* **2**, 17100 (2017).
- 465 23. Helaine, S., Dyer, D. H., Nassif, X., Pelicic, V. & Forest, K. T. 3D structure/function analysis of
466 PilX reveals how minor pilins can modulate the virulence properties of type IV pili. *Proc. Natl.*
467 *Acad. Sci. U. S. A.* **104**, 15888–15893 (2007).
- 468 24. Kolappan, S. *et al.* Structure of the *Neisseria meningitidis* Type IV pilus. *Nat. Commun.* **7**, 13015
469 (2016).
- 470 25. Loeb, T. Isolation of a bacteriophage specific for the F plus and Hfr mating types of *Escherichia*
471 *coli* K-12. *Science.* **131**, 932–933 (1960).
- 472 26. McCutcheon, J. G., Peters, D. L. & Dennis, J. J. Identification and characterization of type IV pili
473 as the cellular receptor of broad host range *Stenotrophomonas maltophilia* bacteriophages DLP1
474 and DLP2. *Viruses* **10**, E338 (2018).
- 475 27. Hu, D. & Reeves, P. R. The remarkable dual-level diversity of prokaryotic flagellins. *mSystems* **5**,

- 476 (2020).
- 477 28. Berube, P. M. *et al.* Single cell genomes of *Prochlorococcus*, *Synechococcus*, and sympatric
478 microbes from diverse marine environments. *Sci. data* **5**, 180154 (2018).
- 479 29. Villar, E. *et al.* The Ocean Gene Atlas: exploring the biogeography of plankton genes online. *Nucleic
480 Acids Res.* **46**, W289–W295 (2018).
- 481 30. Laurenceau, R. *et al.* Toward a genetic system in the marine cyanobacterium *Prochlorococcus*.
482 *Access Microbiol.* **2**, (2020).
- 483 31. Coe, A. *et al.* Survival of *Prochlorococcus* in extended darkness. *Limnol. Oceanogr.* **61**, 1375–1388
484 (2016).
- 485 32. Stocker, R. & Seymour, J. R. Ecology and physics of bacterial chemotaxis in the ocean. *Microbiol.
486 Mol. Biol. Rev.* **76**, 792–812 (2012).
- 487 33. Moore, L. R. *et al.* Culturing the marine cyanobacterium *Prochlorococcus*. *Limnol. Oceanogr.*
488 *Methods* **5**, 353–362 (2007).
- 489 34. Kovach, M. E. *et al.* Four new derivatives of the broad-host-range cloning vector pBBR1MCS,
490 carrying different antibiotic-resistance cassettes. *Gene* **166**, 175–176 (1995).
- 491 35. Kvitko, B. H. & Collmer, A. Construction of *Pseudomonas syringae* pv. tomato DC3000 mutant
492 and polymutant strains. *Methods Mol. Biol.* **712**, 109–128 (2011).
- 493 36. Font-Muñoz, J. S. *et al.* Collective sinking promotes selective cell pairing in planktonic pennate
494 diatoms. *Proc. Natl. Acad. Sci.* **116**, 15997–16002 (2019).
- 495 37. Crocker, J. C. & Grier, D. G. Methods of digital video microscopy for colloidal studies. *J. Colloid
496 Interface Sci.* **179**, 298–310 (1996).
- 497 38. Christie-Oleza, J. A. & Armengaud, J. In-depth analysis of exoproteomes from marine bacteria by
498 shotgun liquid chromatography-tandem mass spectrometry: the *Ruegeria pomeroyi* DSS-3 case-
499 study. *Mar. Drugs* **8**, 2223–2239 (2010).
- 500 39. Christie-Oleza, J. A., Scanlan, D. J. & Armengaud, J. ‘You produce while I clean up’, a strategy
501 revealed by exoproteomics during *Synechococcus-Roseobacter* interactions. *Proteomics* **15**, 3454–
502 3462 (2015).
- 503 40. Cox, J. & Mann, M. MaxQuant enables high peptide identification rates, individualized p.p.b.-range
504 mass accuracies and proteome-wide protein quantification. *Nat. Biotechnol.* **26**, 1367–1372 (2008).
- 505 41. Tyanova, S. *et al.* The Perseus computational platform for comprehensive analysis of (prote)omics
506 data. *Nat. Methods* **13**, 731–740 (2016).
- 507 42. Seemann, T. Prokka: rapid prokaryotic genome annotation. *Bioinformatics* **30**, 2068–2069 (2014).
- 508 43. Okonechnikov, K., Golosova, O. & Fursov, M. Unipro UGENE: a unified bioinformatics toolkit.
509 *Bioinformatics* **28**, 1166–1167 (2012).

- 510 44. Mistry, J., Finn, R. D., Eddy, S. R., Bateman, A. & Punta, M. Challenges in homology search:
511 HMMER3 and convergent evolution of coiled-coil regions. *Nucleic Acids Res.* **41**, e121–e121
512 (2013).
- 513 45. Yang, J. & Zhang, Y. Protein structure and function prediction using I-TASSER. *Curr. Protoc.*
514 *Bioinforma.* **52**, 5.8.1-5.8.15 (2015).

515
516

517 **Acknowledgments**

518 We thank Dr Bakker and the Advanced Bioimaging Platform as well as Dr Hernandez-Fernaund and the
519 WPH Proteomic Facility, at the University of Warwick, for respective support in imaging and proteomics.
520 We thank Dr Guillonneau for providing the protist cultures and WISB centre (grant ref. BB/M017982/1)
521 for access to equipment. This work was supported by NERC grant NE/K009044/1, Ramón y Cajal contract
522 RYC-2017-22452 and the MINECO project CTM2015-70180-R.

523

524 **Author contribution**

525 JC-O conceived the study. MA-F generated the knockout mutant. JC-O and MA-F performed the sinking
526 experiments. VZ, AC and DS performed the proteomic analyses. JC-O, RB and RJP performed the
527 bioinformatics analyses. ML and MP carried out the tracking and imaging of sinking cells. JC-O and MA-
528 F wrote the manuscript with large input from DJS and RJP.

529

530 **Competing interests**

531 The authors declare no competing interests.

532

533 **Data and materials availability:** All detailed methods and data is available as supplementary information
534 and Tables. The mass spectrometry proteomics data have been deposited in the ProteomeXchange
535 Consortium via the PRIDE partner repository with the dataset identifiers: PXD018394, PXD018395,
536 PXD018396, PXD018524 and PXD019315.

537

538 **Supplementary Information**

539 Protocol for generating mutants in marine *Synechococcus*

540 Extended data Table M1 and Figures S1 to S4

541 Extended data Tables S1 to S7

542 Extended data movies 1 to 4